Energy exchange and water budget partitioning in a boreal minerogenic mire

Matthias Peichl,[1] Jörgen Sagerfors,[1] Anders Lindroth,[2] Ishi Buffam,[1,3] Achim Grelle,[4] Leif Klemedtsson,[5] Hjalmar Laudon,[1] and Mats B. Nilsson[1]

Received 14 May 2012; revised 4 December 2012; accepted 8 December 2012; published 18 January 2013.

[1] This study investigated patterns and controls of the seasonal and inter-annual variations in energy fluxes (i.e., sensible heat, H, and latent heat, λE) and partitioning of the water budget (i.e., precipitation, P; evapotranspiration, ET; discharge, Q; and soil water storage, ΔS) over five years (2001–2005) in a boreal oligotrophic fen in northern Sweden based on continuous eddy covariance, water table level (WTL), and weir measurements. For the growing season (May 1 to September 31), the 5 year averages ($\pm$ standard deviation) of the midday (10:00 to 14:00 h) Bowen ratio (β, i.e., $H/\lambda E$) was 0.86 ± 0.08. Seasonal and inter-annual variability of β was mainly driven by λE which itself was strongly controlled by both weather (i.e., vapor pressure deficit, D, and net radiation, R_n) and physiological parameters (i.e., surface resistance). During the growing season, surface resistance largely exceeded aerodynamic resistance, which together with low mean values of the actual ET to potential ET ratio (0.55 ± 0.05) and Priestley-Taylor α (0.89) suggests significant physiological constrains on ET in this well-watered fen. Among the water budget components, the inter-annual variability of ET was lower (199 to 298 mm) compared to Q (225 to 752 mm), with each accounting on average for 34 and 65% of the ecosystem water loss, respectively. The fraction of P expended into ET was negatively correlated to P and positively to R_n. Although a decrease in WTL caused a reduction of the surface conductance, the overall effect of WTL on ET was limited. Non-growing season (October 1 to April 30) fluxes of H, λE, and Q were significant representing on average -67%, 13%, and 61%, respectively, of their growing season sums (negative sign indicates opposite flux direction between the two seasons). Overall, our findings suggest that plant functional type composition, P and R_n dynamics (i.e., amount and timing) were the major controls on the partitioning of the mire energy and water budgets. This has important implications for the regional climate as well as for ecosystem development, nutrient, and carbon dynamics.

Citation: Peichl, M., J. Sagerfors, A. Lindroth, I. Buffam, A. Grelle, L. Klemedtsson, H. Laudon, and M. B. Nilsson (2013), Energy exchange and water budget partitioning in a boreal minerogenic mire, *J. Geophys. Res. Biogeosci.*, *118*, 1–13, doi:10.1029/2012JG002073.

1. Introduction

[2] Peatland ecosystems represent 10–20% of the boreal landscape in Canada, Russia, and Scandinavia and are one of the major constituents of the boreal biome, thus making a notable contribution to the land surface control of the regional climate [*Eugster et al.*, 2000; *Paavalainen and Päivinen*, 1995]. The prerequisite for the existence of peatland ecosystems is a positive water balance which, in turn, is intimately connected to the peatland energy balance [*Ivanov*, 1981]. Both mire (i.e., natural peatland not affected by human activities) type and micro-topography exert controls on the energy and water balance partitioning [*Belyea and Clymo*, 2001; *Bridgham et al.*, 1999; *Nungesser*, 2003]. Moreover, the inter-annual variability of the water balance affects the development and maintenance of mires [*Lafleur et al.*, 2005; *Pastor et al.*, 2002].

[3] The radiation balance and partitioning of energy into latent and sensible heat fluxes are major determinants of regional climate and hydrology [*Eugster et al.*, 2000; *Rouse*, 2000]. The energy from net radiation (R_n) absorbed by the surface is partitioned into latent heat flux (λE) in form of evapotranspiration (ET) of water, sensible heat flux (H),

[1]Department of Forest Ecology and Management, Swedish University of Agricultural Sciences, Umeå, Sweden.
[2]Department of Physical Geography and Ecosystems Analysis, University of Lund, Lund, Sweden.
[3]Department of Biological Sciences, University of Cincinnati, Cincinnati, Ohio, USA.
[4]Department of Ecology, Swedish University of Agricultural Sciences, Uppsala, Sweden.
[5]Department of Plant and Environmental Sciences, University of Gothenburg, Gothenburg, Sweden.

Corresponding author: M. Peichl, Swedish University of Agricultural Sciences, Department of Forest Ecology and Management, SE-90183 Umeå, Sweden. (Matthias.Peichl@slu.se)

2169-8953/13/2012JG002073

and the soil heat flux (G). While λE commonly causes a cooling of the surface and the overlaying atmospheric layer, H and G may exert both warming and cooling effects depending on diurnal and seasonal cycles in energy supply and subsequent temperature differences between soil and near-surface atmospheric layers. Since different mechanisms are likely to be involved in different mire systems, depending on the interactions among water, nutrient availability, and vegetation composition, a good understanding of the controls on these fluxes is essential for accurate climate and ecosystem modeling.

[4] Sphagnum mosses constitute the single most important peat-forming plant genera and differ from vascular plants in their way of obtaining and transporting water which relies primarily on capillary forces determined by atmospheric evaporative demand and the organization of the sphagnum leaves [*Rice et al*., 2001; *Rydin and McDonald*, 1985a, 1985b]. Sphagnum growth and functioning is therefore especially sensitive to changes in micro-topography, water table level, and *ET* rates as well as the frequency and intensities of precipitation events [*Nordbakken*, 1996; *Robroek et al*., 2009; *Rydin and McDonald*, 1985a, 1985b]. In contrast, vascular plants have the ability to control transpiration through gradual closure of their stomata if the atmospheric demand exceeds water supply [*Schulze et al*., 1994]. However, despite this knowledge, there is still considerable uncertainty about the dynamics and contributions from moss and vascular plant transpiration on *ET* in peatland ecosystems [*Lafleur*, 2008].

[5] The water table level (*WTL*) is one of the key control parameters of the mire ecosystem functions since it varies considerably among microtopographical units within mires as well as among mire types [*Belyea and Baird*, 2006; *Belyea and Clymo*, 2001]. Since mosses and vascular plants have different mechanisms controlling their water uptake and loss, their ability to conduct water may behave differently with changes in *WTL* [*Admiral et al*., 2006; *Kurbatova et al*., 2002]. Uncertainty about the role of *WTL* as control on *ET* still also exists. Whereas previous studies reported *WTL* effects on *ET* [*Kellner*, 2001; *Kim and Verma*, 1996], more recent studies come to the conclusion that the response of *ET* to *WTL* is insignificant over a wide range of *WTL* [e.g., *Humphreys et al*., 2006; *Sonnentag et al*., 2010; *Sottocornola and Kiely*, 2010; *Wu et al*., 2010]. On the other hand, it has also been shown that *WTL* is strongly controlled by *ET* [*Lafleur*, 2008; *Wu et al*., 2010]. It is therefore essential to understand the interactions and feedbacks between water and energy exchanges and the *WTL* as it affects the mire vegetation composition and ability to accumulate nutrients and carbon [*Eppinga et al*., 2010; *Flanagan and Syed*, 2011; *Lafleur*, 2008; *Lafleur et al*., 1997, 2005].

[6] To date, only few studies on energy and water exchanges in peatlands exist with complete annual data series over multiple (i.e., ≥5) years [*Lafleur*, 2008; but see *Lafleur et al*., 2005; *Sottocornola and Kiely*, 2010]. However, such data sets are required to understand the contribution of different seasons (specifically the winter season in northern boreal regions) to the annual water and energy partitioning and the controls on its inter-annual variability [*Lafleur*, 2008; *Williams et al*., 2012]. Furthermore, previous micrometeorological studies of peatland energy exchanges commonly focused on investigating patterns of evapotranspiration during the growing season [*Humphreys et al*., 2006; *Lafleur*, 2008], whereas little attention has been paid to dynamics of the sensible heat flux, non-growing season fluxes and to understanding the complete water budget partitioning (i.e., including the discharge) [but see, e.g., *Lafleur et al*., 2005; *Wu et al*., 2010].

[7] Based on multi-year continuous eddy-covariance measurements of energy and water fluxes, water discharge, and water table level, the aims of this study were (i) to determine seasonal patterns and inter-annual variability of sensible/latent heat fluxes and the water budget components, (ii) to identify the main controls on the variability of energy exchanges and water balance partitioning, and (iii) to determine the role of non-growing season energy and water fluxes in a boreal fen in northern Sweden. Our three main hypotheses are that (i) the seasonal and inter-annual variability of energy partitioning is driven by patterns of the λE flux which itself is regulated mainly by atmospheric but also by vegetation controls, (ii) the timing and magnitude of precipitation combined with the concurrent water table level determine the partitioning of precipitation into the water budget components evapotranspiration and discharge, and (iii) non-growing season energy and water fluxes constitute a significant portion of the annual exchange in this northern boreal peatland.

2. Materials and Methods

2.1. Site description

[8] The study was conducted at Degerö Stormyr, (64°11′N, 19°33′E), an acid, oligotrophic, minerogenic, mixed mire system covering 6.5 km^2 and situated in the Kulbäcksliden research park of the Svartberget Long-Term Experimental Research (LTER) facility near the town of Vindeln, county of Västerbotten, Sweden. The mire area, which consists of a rather complex system of interconnected smaller mires divided by islets and ridges of glacial till, is situated on a highland 270 m above sea level between two major rivers, Umeälven and Vindelälven, approximately 70 km from the Gulf of Bothnia. The depth of the peat is generally between 3 and 4 m, but depths up to 8 m have been measured. The deepest peat layers correspond to an age of ~8000 years. The mire catchment is predominantly drained by the small creek Vargstugbäcken.

[9] The micro-topography within the footprint area is predominantly an irregular two-phase mosaic of carpets and lawns, with only sparse occurrences of hummocks. The vascular plant community of the mire consists mainly of *Eriophorum vaginatum* L., *Trichophorum cespitosum* L. Hartm., *Vaccinium oxycoccos* L., *Andromeda polifolia* L., *Rubus chamaemorus* L. with both *Carex limosa* L., and *Schezeria palustris* L. occurring more sparsely. In addition, *Sphagnum majus* Russ. C. Jens is found on the bottom of the carpets, while *S. lindbergii* Schimp. and *S. balticum* Russ. C. Jens are common for the lawns. The hummocks are dominated by *S. fuscum* Schimp. Klinggr. and *S. rubellum* Wils [*Laine et al*., 2012; *Nilsson et al*., 2008]. Total (moss + vascular plants) area weighted average aboveground biomass within the flux tower footprint is $141 \pm 45\ g \cdot m^{-2}$ [*Laine et al*., 2012].

[10] The 30 year (1961–1990) mean annual precipitation and temperature are 523 mm and +1.2 °C, respectively, while the mean temperatures in July and January are +14.7 °C and −12.4 °C, respectively [*Alexandersson et al*., 1991]. The length of the vegetation period (defined as the period during which the mean daily temperature remains

above +5 °C) over the recording period (2001–2005) was 156 ± 15 days. The snow cover normally reaches a depth of up to 0.6 m and lasts for approximately 6 months.

[11] The dominant wind direction during the summer is North-East, while in the winter, the prevailing wind is from the South-East. Based on the Schmid footprint model [*Schmid*, 1994], the footprint area (95% percentile of the source distance) around the tower covers a radius of 22 m (daytime) to 74 m (nighttime) during the summer and about 76 m (day and nighttime) during the winter, although the distance from the tower to the peak source area is much less according to the plot of the cumulated fetch distances [*Sagerfors et al*., 2008]. During wintertime the measuring height (z_m) of 1.8 m was maintained by stepwise rising of the boom to account for the accumulation of snow.

2.2. Air and soil environmental measurements

[12] Instruments for measurements of environmental variables were mounted on the same tower as the eddy-covariance sensors. Net radiation (R_n) and global radiation (R_g) were measured using a NR-Lite sensor (Kipp&Zonen, Delft, the Netherlands) and a Li200sz sensor (LICOR, Lincoln, Nebraska, USA), respectively, mounted at the top of the tower (i.e., 4 m above the ground). The NR-Lite sensor was calibrated annually and cross-checked to ensure consistency and quality of the measurements. In addition, air temperature (T_a) and relative humidity (h) were measured by a MP100 temperature and moisture sensor (Rotronic AG, Bassersdorf, Switzerland) inside a self-ventilated radiation shield mounted 1.8 m above the ground. The T_a and h data were used to derive the atmospheric vapor pressure deficit (D). All environmental data were collected at 10 s intervals. Rainfall was measured using a tipping-bucket (ARG 100, Campbell Scientific, Logan, Utah, USA) 4 m away from the tower during April to October and corrected for a (10%) underestimation of the precipitation [*Eriksson*, 1983]. During the remaining period, precipitation data were obtained from a nearby (1 km away) meteorological station at Kulbäcksliden, where the snowfall was melted once a week to estimate the snow water equivalent. The snow depth at the study site was measured by an SR-50 ultrasonic sensor (Campbell Scientific, Logan, Utah, USA) placed approximately 6 m from the flux tower. Gaps in environmental variables (due to instrument failure) and the period between October 1 and December 31 in 2000 (to obtain an annual sum for the hydrological year 2000/2001) were filled either directly (i.e., for P) or with seasonal regression relationships (i.e., for T_a, R_n, and h) with respective data from the nearby (13 km away) meteorological station at the Svartberget Research Station.

[13] The water table level below the peat surface was measured in a lawn community 100 m northeast of the flux tower. The difference between peat surface and water table level was determined using a float and counterweight system attached to a potentiometer [*Roulet et al*., 1991]. All environmental data were averaged and stored as 30 min mean values on a data logger (CR10X, Campbell Scientific, Logan, Utah, USA).

2.3. Eddy-covariance measurements

[14] The eddy-covariance (EC) technique was used to measure the fluxes of heat, water vapor, and momentum at a sampling frequency of 20 Hz. The system consisted of a three-dimensional sonic anemometer (model 1012R2 Solent, Gill Instruments, UK) and a closed-path infrared gas analyzer (IRGA model 6262, LI COR, Lincoln, Nebraska USA) supplied by In Situ Flux Systems AB, Sweden. The IRGA was mounted in a climate-controlled instrument box approximately 3 m south of the air intake. The air intake was less than 5 cm from the measuring volume of the sonic anemometer. The air pump was placed behind the IRGA to suck the air through the analyzer, which was connected to the intake through a 5 m long tubing with a 4 mm inner diameter. A particle filter (Acro®50 1 µm PTFE, Pall Gelman Laboratory, Ann Arbor, Michigan, USA) was positioned between the intake and the IRGA. The sonic anemometer was mounted on the tower at a height of 1.8 m on a 1.0 m long boom and heated during the winter months. Fluxes were calculated in real time by the EcoFlux software (In Situ Flux AB, Ockelbo, Sweden) according to the EUROFLUX methodology [*Aubinet et al*., 1999] and stored as 30 min averages. Raw data processing included a coordinate correction by planar fit and a frequency correction for the signal attenuation in the sampling path. Systematic errors are commonly assumed to be in the range of 10–20% for any individual half-hourly turbulent flux measurement but usually decrease to less than 10% when aggregated over longer time scales due to canceling effects [*Moncrieff et al*., 1996; *Morgenstern et al*., 2004]. The H_2O concentration was calibrated retrospectively against the water vapor concentration obtained from a ventilated Rotronic sensor (MP100, Rotronic AG, Bassersdorf, Switzerland). The Rotronic was in turn calibrated regularly using an aspirated psychrometer (Assman, type 761, Wilhelm Lambrecht Gmbh, Göttingen, Germany). When the water vapor measurements from the gas analyzer deviated from the Rotronic measurements, the gas analyzer values were post processed and the fluxes corrected accordingly. A typical calibration interval for H_2O was 3–4 weeks.

[15] Missing half hourly, H and λE data points (due to instrument and power failure, etc.) were filled following *Amiro et al*. [2006] to obtain annual budgets. Filled data represented 35, 20, 32, 35, and 27% of the annual time series in 2001 to 2005, respectively. For the hydrological year 2000/2001, H and λE fluxes for October 1 to December 31 in 2000 were estimated from the average of the respective period over the years 2001 to 2005. Fluxes directed towards the surface were recorded as negative values while fluxes away from the surface were positive.

2.4. Actual and potential evaporation

[16] Actual evapotranspiration (ET) was estimated by dividing the measured latent heat flux by the latent heat of vaporization. Potential evapotranspiration (PET) was estimated by two methods: the Penman-Monteith equation [*Monteith*, 1965] and the Priestley-Taylor equation [*Priestley and Taylor*, 1972]. Using the former and assuming the surface resistance (r_s) to be zero, PET was estimated as

$$PET = \frac{A\cdot\Delta + \frac{\rho\cdot Cp\cdot\delta e}{r_a}}{(\Delta+\gamma)\cdot L_v} \quad (1)$$

where Δ is the slope of vapor pressure saturation versus temperature curve [Pa K^{-1}], γ is the psychrometric constant = 66 [Pa K^{-1}], ρ is air density [g m^{-3}], C_p is the specific heat capacity of air at constant pressure [J g^{-1}], δe is the saturation vapor pressure deficit at air temperature [Pa], r_a is the

aerodynamic resistance [s m^{-1}] (see section 2.5), and L_v is the specific heat of vaporization [J g^{-1}]. A is available energy (R_n – G) [W m^{-2}]; however, here we set A equal to net radiation, R_n, since equation 1 was solved on a daily time scale at which soil heat flux, G, is normally a few percent of the net radiation [*Kellner*, 2001] and thus may be neglected.

[17] The Priestley-Taylor ET was estimated from the equilibrium evaporation, λE_{eq}:

$$\lambda E_{eq} = \frac{\Delta}{\Delta + \gamma}(A) \tag{2}$$

then the Priestley-Taylor coefficient, α, was estimated from the ratio of actual ET to λE_{eq} (equation (3)).

$$\alpha = \frac{ET}{\lambda E_{eq}} \tag{3}$$

2.5. The aerodynamic resistance

[18] The aerodynamic resistance, r_a, for transfer of heat and water vapor from the surface to the reference level was estimated based on equation (4) [*Verma*, 1989]:

$$r_a = \left[\frac{u(z)}{u_*^2}\right] + \left[\frac{\ln(z_0/z_{0t})}{k \cdot u_*}\right] \tag{4}$$

where $u(z)$ is the wind speed at the reference height z measured by the sonic anemometer, u_* is the friction velocity, z_0 is the roughness length for wind, z_{0t} is the roughness length for temperature, and k is the von Karman's constant. The first term on the right-hand side of equation (4) is the aerodynamic resistance to momentum transfer, and the second term is the so called excess resistance which considers the extra resistance due to the difference in transfer for momentum and heat/water vapor [*Mölder and Kellner*, 2002; *Verma*, 1989]. Moreover, here it is assumed that the resistances for heat and water vapor transfer are equal. Since there were no measurements of temperature profiles and surface temperature, it was not possible to calculate z_{0t} directly. For a low surface and neglecting the stratification effects, we followed the approach by *Mölder and Kellner* [2002]:

$$\ln(z_0/z_{0t}) = 1.58 \cdot \mathrm{Re}_0{}^{0.25} - 3.4 \tag{5}$$

where Re_0 is the roughness Reynolds number:

$$\mathrm{Re}_0 = z_0 \cdot u_* / v \tag{6}$$

where v, the viscosity of air, was assumed constant at 1.81×10^{-5} kg m^{-1} s^{-1} at 15 °C. The roughness length for wind, z_0, was estimated from solving equation (7) for z_0:

$$u(z) = \frac{u_*}{k} \cdot \ln(z/z_0) \tag{7}$$

[19] The estimation of z_0 was made during near neutral conditions ($-0.1 < z/L < 0.1$; where L is the Monin-Obukhov stability length).

2.6. Surface resistance and conductance

[20] During conditions when the vegetation surfaces are not completely wet, the transport of water vapor into the atmosphere experiences, besides the aerodynamic resistance, an additional resistance denoted surface resistance (r_s). However, while r_s describes constraints on evapotranspiration in the context of turbulent land-atmosphere exchanges, the surface conductance (g_s) as the reciprocal of r_s is commonly used to describe the ability of vegetation to transport and transpire water from the below the surface to the atmosphere. To be able to better compare our results with those from previous studies, we therefore computed both r_s and g_s from the inverse of the Penman-Monteith equation as:

$$g_s = \frac{A \cdot \gamma}{\rho \cdot Cp \cdot \delta e \cdot (1 + \beta) + A \cdot (\Delta \cdot \beta - \gamma) \cdot r_a} \tag{8}$$

g_s was calculated for the daytime, 0800–1800 h, and during precipitation-free periods, defined as times when no precipitation had occurred for at least 24 h before the measurements. On the half-hourly time scale used in the calculations of g_s, the assumption previously made in equation (1) (stating that A equals R_n on a daily time scale) is invalid and leads to an overestimation of A and g_s. To compensate for this, we reduced R_n by 10% to obtain a better estimate of A. The correction factor was based on a study in another Swedish mire (Stormossen) which found that G was 10% of R_n and closely followed its diurnal variation [*Kellner*, 2001].

[21] To reveal any possible effect of systematic errors on flux measurement performance, we determined the energy balance closure as the difference between the sum of the turbulent energy fluxes ($H + \lambda E$), as measured by the eddy-covariance system, and the available energy (i.e., $R_n - G$). However, since G was not measured explicitly, the energy balance closure was determined on an annual basis at which scale the soil heat flux can be considered negligible, in two ways: (i) against R_n only and (ii) against $R_n - G$ where G was estimated as 10% of R_n [*Kellner*, 2001].

2.7. Catchment discharge estimates

[22] A first estimate of annual mire discharge (Q) was obtained from the residual of the water balance for the hydrological years October 2001 to September 2005 as followed:

$$Q = P - ET + \Delta S \tag{9}$$

where P is the annual water input via precipitation, ET is evapotranspiration measured with the EC method, and ΔS is the change in soil water storage. ΔS was derived from the difference in WTL relative to the mire surface between 1 October and 30 September of consecutive years, assuming an average peat porosity of 0.90. During the growing season, shrinking and swelling processes may considerably alter mire surface elevation and thus estimates of ΔS based on WTL need to be corrected accordingly on such time scale [*Barr et al.*, 2012]. On the annual scale, however, surface elevation changes may be considered rather small. Continuous data from the SR-50 ultrasonic snow sensor (anchored into the underlying mineral soil) during the summer 2005 and from more recent years (unpublished data) suggest a limited change (~2 cm) in mire surface elevation over a full year. Since continuous snow sensor data were not available during the summer of the other study years, we did not correct the relative WTL by changes in surface elevation. We estimate that this approach introduced an error of ±20 mm to the ΔS term.

[23] For comparison, Q was also estimated using discharge measurements at the catchment outlet for the hydrological years 2002/2003 to 2004/2005 [*Nilsson et al.*, 2008]. Subcatchment boundary delineation for the 3.1 km^2 catchment of Vargstugbäcken (~50% of the total mire catchment (6.5 km^2)) was determined based on field observations and a 50 m grid digital elevation model (DEM) using IDRISI 14 (Clark Labs, Worcester, MA, USA). Hourly stream discharge was calculated using measurements of stream stage from water height loggers (wt-hr logger, Trutrack Inc., New Zealand) at a V-notch weir and an established height-discharge rating curve ($r^2 = 0.99$). Stream stage measurements were not available for 45% of the time, mainly during winter low flow conditions when the weir was not yet heated and ice and temperatures below freezing point made stage measurements unreliable. During these periods, stream flow was estimated using a calibrated ratio of flow between this site and a reference site at the Svartberget catchment, Krycklan, 10 km north at which flow was measured at a V-notch weir in a heated dam house [*Ågren et al.*, 2007]. Because gap filling was required primarily during very low flow periods, this only represented 16% of the total Q. The measured total discharge (Q_T) was the sum of discharge from the mire (Q_M) and adjacent upland forest (Q_F) (equation (10a)). The source area (A_T) of Q_T was to 69% constituted by the mire (A_M) and to 31% by the forest (A_F). The forest specific discharge (Qs_F) was taken from weir measurements carried out in the nearby forest catchment at Svartberget [*Ågren et al.*, 2007]. The mire specific discharge (Qs_M) was then estimated by solving equations (10b) and (10c):

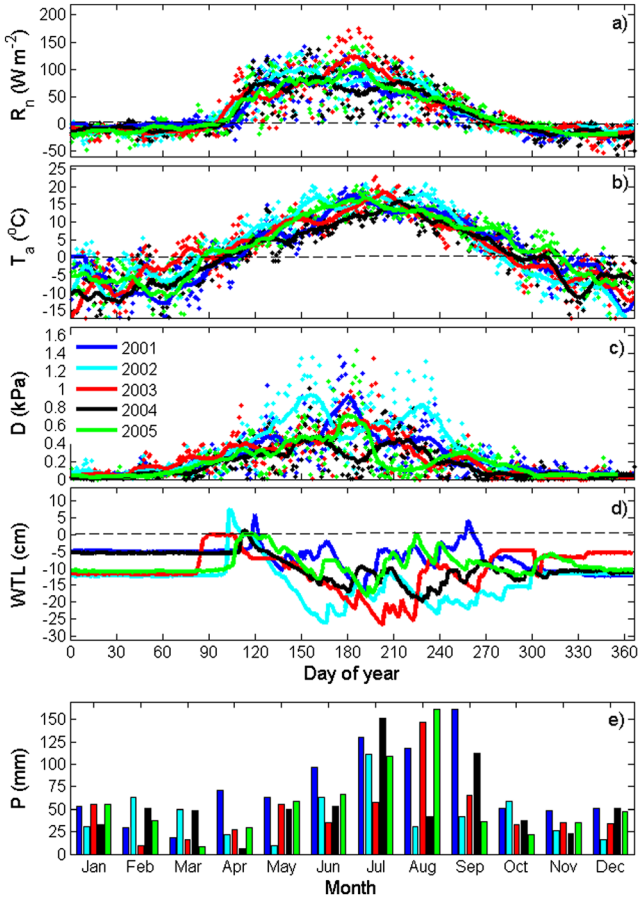

Figure 1. Daily (symbols) means of (a) net radiation (R_n), (b) air temperature (T_a), (c) vapor pressure deficit (D) and (d) water table level (WTL), and (e) monthly sums of precipitation (P) in the years 2001 to 2005; solid lines in Figures 1a–1c (i.e., R_n, T_a, and D) show a 21 day running average. Dashed lines indicate the y axis zero line.

$$Q_T = Q_M + Q_F \tag{10a}$$

$$\frac{Q_F}{Q_M} = \frac{Qs_F}{Qs_M} \times \frac{A_F}{A_M} \tag{10b}$$

$$Qs_M = \frac{Qs_F \times (Q_T - Q_F) \times 0.31}{Q_F \times 0.69} \tag{10c}$$

3. Results

3.1. Environmental conditions

[24] Compared to other years, 2002 had the highest T_a in spring and late summer whereas 2004 was the year with the coldest summer (Figure 1 and Table 1). Corresponding to the seasonal patterns in T_a, peak D values occurred in spring and late summer of 2002 (Figure 1). Furthermore, periods with high D corresponded with a decrease in WTL in all years. The monthly totals of P were generally higher during late summer compared to the remaining seasons. The 2001 growing season was the wettest (570 mm) and had the highest mean WTL (−6.5 cm), while the 2002 growing season was the driest (260 mm) with the lowest mean WTL (−17.6 cm) among years (Table 1).

3.2. Mire surface characteristics

3.2.1. Surface roughness length

[25] The roughness length (z_0) of the mire surface showed a clear seasonal trend coinciding with vegetation growth

Table 1. Growing Season (GS, 1 May to 30 September) Means of Net Radiation (R_n), Air Temperature (T_a), Vapor Pressure Deficit (D), Precipitation (P), Water Table Level (WTL), Midday (10:00 to 14:00) Bowen Ratio (β), Daytime (0800–1800 h) Evaporative Fraction ($\lambda E/R_n$), the Priestley-Taylor Coefficient, α, and the Ratio of Actual to Potential Evapotranspiration (ET/PET) for 2001 to 2005

GS	R_n (Wm^{-2})	T_a (°C)	D (kPa)	P (mm)	WTL (cm)	β	$\lambda E/R_n$	α	ET/PET
2001	58	11.2	0.44	570	−6.5	0.88	0.61	1.03	0.59
2002	68	13.3	0.60	260	−17.6	0.76	0.76	1.17	0.53
2003	65	10.8	0.37	364	−14.7	0.78	0.67	0.87	0.60
2004	57	9.3	0.29	408	−12.1	0.92	0.55	0.86	0.49
2005	61	11.6	0.32	433	−8.0	0.94	0.57	0.99	0.54
Mean	62	11.2	0.4	407	−11.8	0.86	0.63	0.98	0.55

during the summer and reached a maximum of approximately 3 cm in the peak growing season (Figure 2a). Despite a common seasonal pattern, considerable inter-annual variability in z_0 occurred. For instance, z_0 values were higher corresponding to higher T_a and R_n (and the likely related development of vascular plant vegetation) in the spring and early summer of 2002 and 2003, compared to other years.

3.2.2. Surface and aerodynamic resistances

[26] The surface resistance (r_s) showed a diurnal decrease during the afternoon corresponding to increases in D (not shown). Furthermore, seasonal patterns in r_s were also driven by D (e.g., compare peaks of D and r_s in 2001 and 2002) resulting in considerable seasonal and inter-annual variability in r_s (Figure 2b). Similar as for z_0, higher r_s was observed during spring and early summer of 2002 and 2003.

[27] The aerodynamic resistance (r_a) showed a diurnal pattern with a decrease during turbulent daytime conditions but, in contrast to r_s, showed no clear seasonal trend or inter-annual variability (not shown, but see Figure 3).

[28] The 5 year averages demonstrate that r_s largely exceeded r_a during the period between snowmelt and winter snowfall (Figure 3). Furthermore, the mean pattern of r_s followed closely that of z_0 throughout the entire growing season but diverged during the vegetation senescence period in autumn.

3.3. Patterns and controls of mire surface-atmosphere energy exchanges

[29] The slope of the regression between R_n and the sum of λE and H as indicator for the energy balance closure

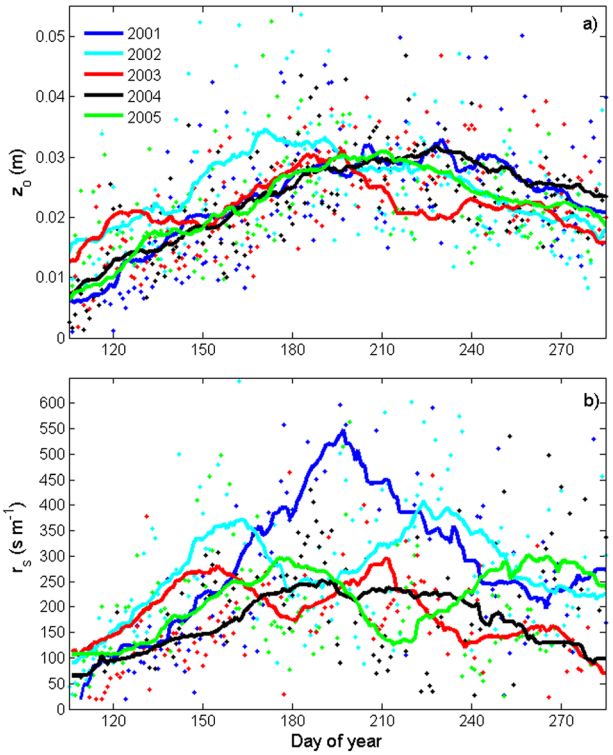

Figure 2. Daily averages (symbols) of (a) surface roughness length (z_0) and (b) surface resistance (r_s) in the snow-free period (mid-April to mid-October) of the years 2001–2005; lines show daily values smoothed with a 30 day running average.

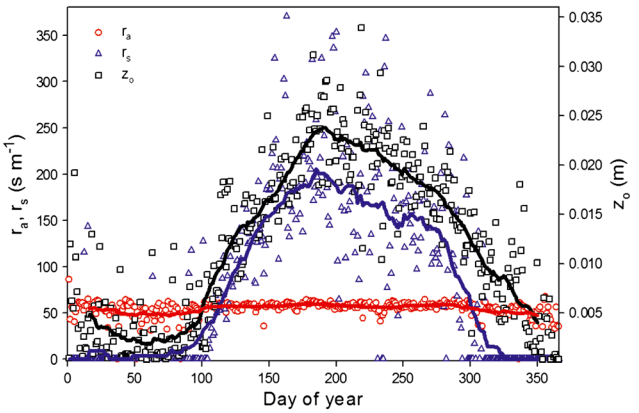

Figure 3. Five year averages of daily means of the aerodynamic (r_a, red symbols) and surface (r_s, blue symbols) resistance and the surface roughness length (z_o, black symbols) based on the years 2001 to 2005. Solid lines represent 21 day smoothing averages to visualize the main seasonal trends.

was 0.90 averaged over the 5 years (Figure 4) and not significantly different among the 5 years (not shown). After adjusting R_n by −10% to account for G, the slope improved to 1.0. Furthermore, the small y axis intercept of 1.47 indicates the absence of systematic bias. These results provide confidence in the quality of the measured energy fluxes at this site.

[30] Daily means of λE reached a maxima of ~90 W m^{-2} and showed considerably inter-annual variation in their seasonal patterns (Figure 5a). Seasonal peaks of λE corresponded to peaks in D (see, e.g., 2002, compare to Figure 1). In the spring and early summer of 2002 and 2003 (recall Figures 1), λE exceeded those of other years during those periods. In comparison to λE, daily means of H were lower (maximum values of ~60 W m^{-2}) and their seasonal and inter-annual variation was limited (Figure 5b).

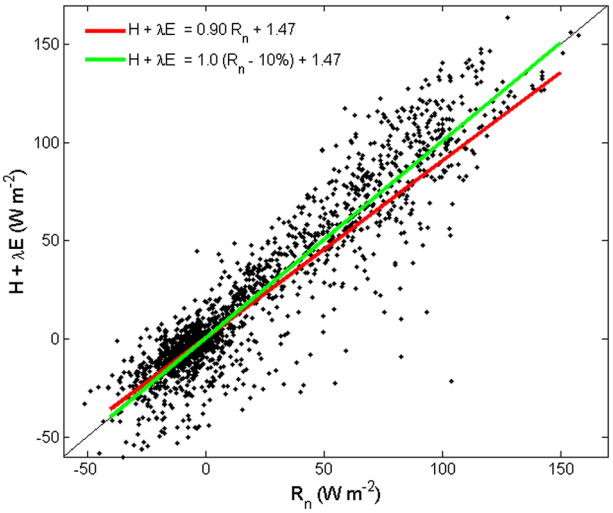

Figure 4. Energy balance closure (*EBC*) derived from the linear slope of the daily sums of mean sensible (H) and latent (λE) heat fluxes regressed against daily mean net radiation (R_n) (black symbols, red regression line; $EBC = 0.90$) and against R_n—10% to account for the ground heat flux (green regression line; $EBC = 1.0$) for the years 2001to 2005.

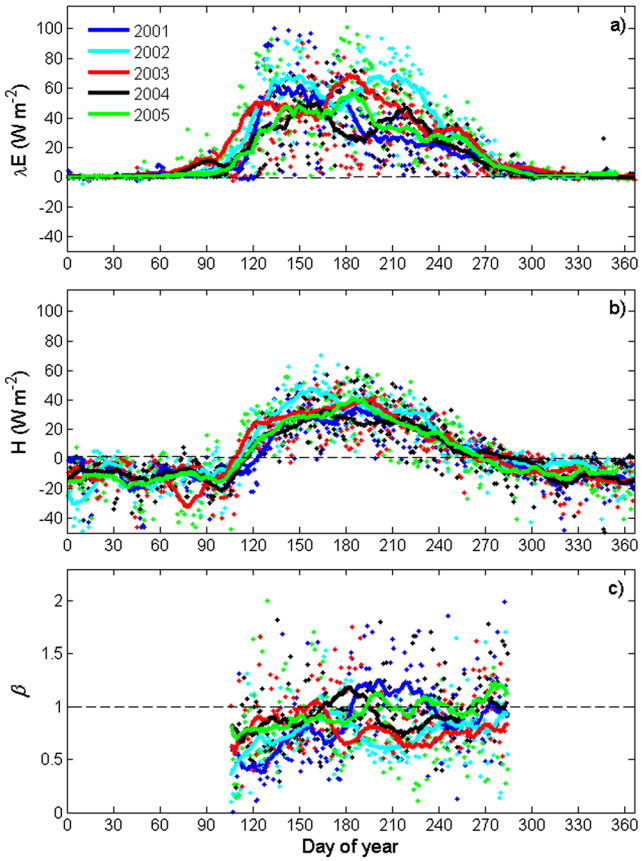

Figure 5. Daily means of (a) latent heat flux (λE), (b) sensible heat flux (H), and (c) midday (10:00 to 14:00 h) Bowen ratio (β) for the snow-free period in the years 2001 to 2005. Solid lines represent 21 day smoothing averages to visualize the main seasonal trends. Dashed lines indicate the y axis zero line in Figures 5a and 5b, and $\beta = 1$ in Figure 5c.

[31] The daily midday Bowen ratio, β, describing the partitioning between H and λE was commonly < 1, except for dry periods with high D (e.g., in summer 2001) during which β values exceeded 1 (Figure 5c). The growing season β was lowest in 2002 and 2003 (0.76 and 0.78, respectively) and highest in 2005 with 0.94, with a 5 year mean of 0.86 ± 0.08 (Table 1). Moreover, daily β increased significantly as *WTL* dropped from 0 to about −10 cm but remained constant once *WTL* was below −10 cm (Figure 6f).

[32] The ratio of daily $\lambda E / R_n$ was on average 61, 76, 67, 55, and 57% for the years 2001 to 2005, respectively (Table 1). Moreover, $\lambda E/R_n$ was positively correlated to growing season D ($r^2 = 0.80$) and R_n ($r^2 = 0.83$).

3.4. Patterns and controls of mire surface to atmosphere transport of water

3.4.1. Evapotranspiration

[33] Evapotranspiration (*ET*) rates at Degerö Stormyr were about 2–3 mm d^{-1} with peak values of close to 4 mm d^{-1}. R_n and D were the main drivers of daily *ET* (Figures 6a and 6b), whereas surface conductance, g_s, had little effect on *ET* (Figure 6c). Daily *ET* remained similar for a *WTL* range of 0 to −15 cm but increased with decreasing *WTL* below −15 cm (Figure 6d). However, a similar relationship between *WTL* and T_a (Figure 6h) suggests cofounding effects among *WTL*, T_a, and *ET*.

[34] Averaged over the five growing seasons, actual *ET* was $55 \pm 5\%$ of *PET* and the Priestley-Taylor α-value was 0.98 ± 12 (Table 1). On the growing season scale, *ET*/*PET* ratio was not correlated to *WTL* while the Priestley-Taylor α-values were positively correlated to D ($r^2 = 0.78$) and T_a ($r^2 = 0.84$). Moreover, daily *ET*/*PET* increased as *WTL* decreased from 0 to about −10 cm but remained constant once *WTL* was below −10 cm (Figure 6e).

3.4.2. Surface conductance

[35] In contrast to the lack of relationship between *ET* and g_s on the daily scale (recall Figure 6c), the diurnal pattern of *ET* was closely related to that of g_s, which reached 35 mm s^{-1} in the morning and then decreased within a few hours to <15 mm s^{-1} (not shown). When averaged over different *WTL* classes, daily g_s decreased from about 9.5 mm s^{-1} at 0 cm to ~3 mm s^{-1} at a *WTL* of 25 cm depth (Figure 6g). Furthermore, g_s was strongly controlled by D, with an additional influence of incoming solar radiation that was most pronounced at D levels lower than ~1.5 kPa (Figure 7).

3.5. Mire water budget

[36] Averaged over 5 (hydrological) years, annual *ET* and Q represented 37% and 65% of the annual precipitation, respectively (Table 2) (with the imbalance in the partitioning resulting from the additional small effect from ΔS). Average Q (462 mm) was about twice that of *ET* (241 mm) and showed greater inter-annual variability (with the coefficient of variation, CV = 37%) compared to *ET* (CV = 16%). The ΔS was also highly variable among years. In 2002/2003 to 2004/2005, independent estimates of ΔS and Q derived either (i) with ΔS from differences in *WTL* (without correction for surface level changes) and Q as residual of the water balance or (ii) with Q from continuous catchment discharge measurements and ΔS as residual of the water balance suggested some difference in 2003/2004 but reasonable agreement in 2002/2003 and 2004/2005. Overall, Q estimates based on the weir measurements were somewhat lower compared to those derived as residual from the water balance (Table 2).

[37] On the growing season scale, the partitioning of precipitation (P) into Q and *ET* correlated with the amount of P, suggesting a strong negative relationship ($r^2 = 0.93$) between P and *ET*/P and conversely a modest positive correlation relationship ($r^2 = 0.55$) of P to Q/P (Figure 8a). Furthermore, *ET*/P and Q/P showed positive ($r^2 = 0.97$) and negative ($r^2 = 0.84$) relationships, respectively, with R_n (Figure 8b). Meanwhile, the total amount of P or R_n did not affect ΔS. Similar relationships for the partitioning of P into Q and *ET* were observed on the annual scale (not shown).

[38] The role of precipitation and *WTL* on seasonal water flux partitioning was investigated during the years 2003 to 2005 in which continuously measured Q data were available. Precipitation and snow melt in early spring (i.e., April and May), when *ET* was low and the underlying soil still frozen, resulted in large discharge fluxes (Figure 9a). During the 2003 summer period with comparably lower *WTL* (i.e., at about −20 cm), precipitation events resulted in raised *WTL* (compare also with Figure 1)

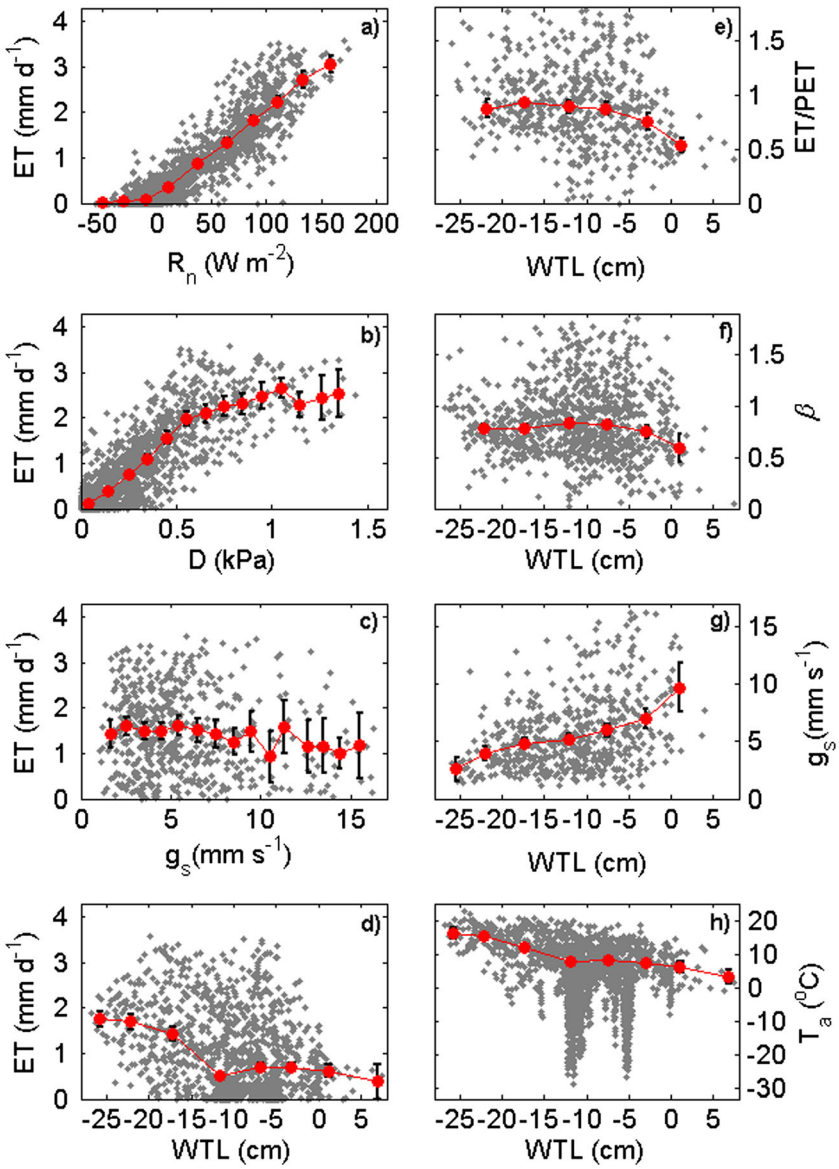

Figure 6. Regression relationships showing (a–d) the response of daily evapotranspiration (*ET*) to net radiation (R_n), vapor pressure deficit (D), surface conductance (g_s) and water table level (*WTL*), and (e–h) *WTL* controls on the ratio of actual to potential *ET* (*ET*/*PET*), Bowen ratio (β), g_s, and air temperature (T_a). Gray symbols show daily values, red symbols show the block-averaged mean response, and black error bars indicate ±2 standard error.

and soil water recharge and hence Q remained low. In comparison, precipitation during summer periods with higher *WTL* (~−10 cm) in 2004 and 2005 (most pronounced in July 2004 and August 2005) triggered considerable discharge fluxes that in some months largely exceeded those of *ET* (Figure 9a). Similarly, rainfall during the autumn, when *WTL* was already relatively high and *ET* reduced due to lower temperatures, resulted in increased Q. The ΔS derived as the residual between precipitation, evapotranspiration, and runoff ($\Delta S = P - ET - Q$) mirrored the temporal variation in *WTL*. Cumulative *ET* initially exceeded Q in the dry year 2002/2003, the following two wet years however caused a switch and Q to became a larger water budget component (~1000 mm) than *ET* (~800 mm) over the entire 3 year period (Figure 9b).

3.6. Non-growing season energy and water fluxes

[39] The 5 year average non-growing to growing season ratio for R_n, P, H, and λE was −0.14, 0.66, −0.67, and 0.13, respectively (Table 3). The negative sign for R_n and H indicates opposite flux directions during the two seasons. The 3 year mean non-growing to growing season ratio for Q was 0.61. However, this ratio was sensitive to the timing of snowmelt (which may occur in either April or May). Q during the snow covered period represented 10% of the annual runoff. The non-growing season *ET* was on average 12% of the annual sum. During the snow covered period, λE was close to zero whereas H was mostly negative, highly variable and closely connected to net radiation (recall Figure 7).

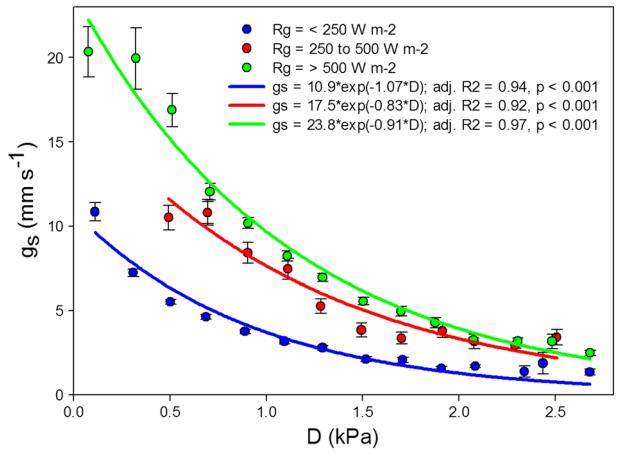

Figure 7. Block-averaged mean response (symbols) and exponential decay curves (solid lines) describing the relationship between surface conductance (g_s) and vapor pressure deficit (D) for different ranges of global radiation (R_g); black error bars indicate ±2 standard error.

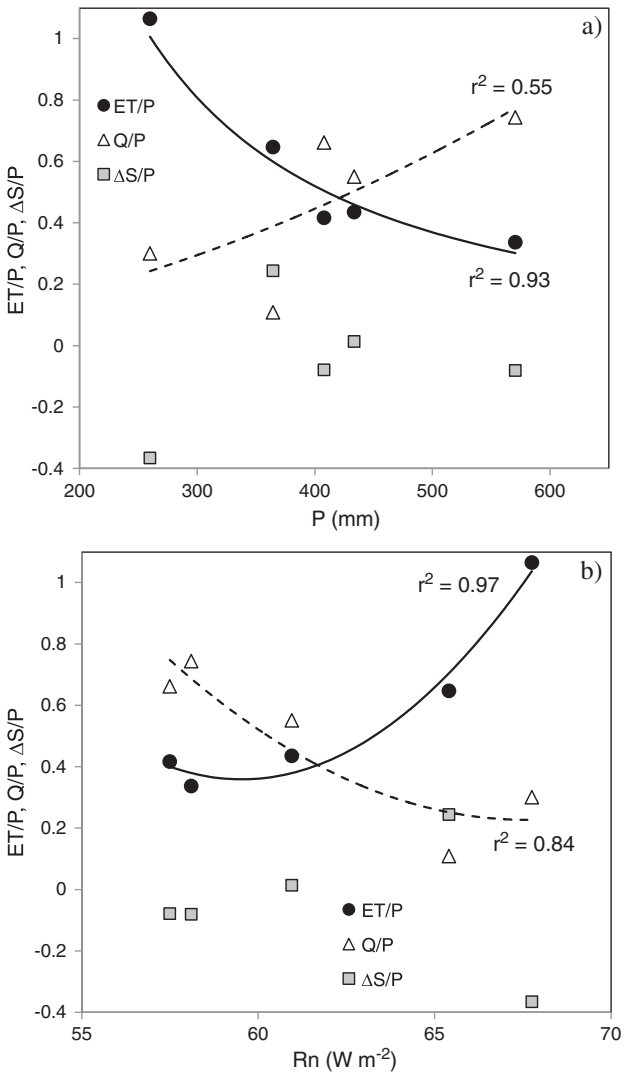

Figure 8. Relationships between growing season (1 May to 30 September) partitioning of precipitation (P) into evapotranspiration (ET/P), discharge (Q/P), and change in soil water storage ($\Delta S/P$) with (a) totals of precipitation (P) and (b) mean net radiation (R_n); solid and dotted lines show power and second-order polynomial fit, respectively.

4. Discussion

4.1. Seasonal and inter-annual variability of mire energy exchange

[40] The greater inter-annual variability in λE compared to H is likely the result from the tight relationship between λE and its atmospheric climate and physiological controls, i.e., D, R_n, and r_s [*Humphreys et al.*, 2006; *Lafleur et al.*, 2005]. λE was especially sensitive to climatic conditions at the onset of the growing season as seen in April of 2002 and 2003 where higher λE was closely linked to greater R_n, T_a, D, and z_0 (reflecting vascular biomass development) relative to other years. In comparison, responses of H to environmental changes remained conservative, mainly because increases in R_n were primarily allocated to λE. This is further corroborated by the negative relationships of β with D and R_n observed in our study. Similarly, *Wu et al.* [2010] found that D and R_n were the main drivers of λE and β in an Eastern Finish mire complex. Thus, in support of our first hypothesis, the growing season β were mainly driven by λE and its direct atmospheric controls, rather than by variations in H.

[41] The range in β (0.76 to 0.94) at the oligotrophic fen Degerö Stormyr is similar to the range of 0.81 and 1.05 in an Irish blanket bog over 5 years [*Sottocornola and Kiely*, 2010]. In contrast, β in our study was higher compared to 0.68 averaged over two growing seasons for an ombrotrophic bog, Stormossen, in Central Sweden [*Kellner*, 2001], despite similar summer *WTL*. In combination with the observed negative correlation between β and R_n, this suggests

Table 2. Annual Totals of the Different Mire Water Balance Components (i.e., Precipitation, P; Evapotranspiration, ET; Discharge, Q, Derived as Residual of the Water Balance; and Soil Water Storage Change, ΔS, Based On Differences in Water Table Level) During the Hydrological Years 2000/2001–2004/2005; Values in Square Brackets Represent Alternative Estimates of Q Derived from Catchment Measurements and of ΔS as the Subsequent Residual of the Water Balance

Year	P (mm)	ET (mm)	Q (mm)	ΔS (mm)	ET/P	Q/P
2000/2001	936	230	752	−46	0.25	0.80
2001/2002	576	298	373	−95	0.52	0.65
2002/2003	587	273	225 [174]	89 [144]	0.46	0.38 [0.30]
2003/2004	665	199	498 [397]	−32 [69]	0.30	0.75 [0.60]
2004/2005	672	205	461 [404]	6 [63]	0.30	0.69 [0.60]
Mean	687	241	462	−16	0.37	0.65

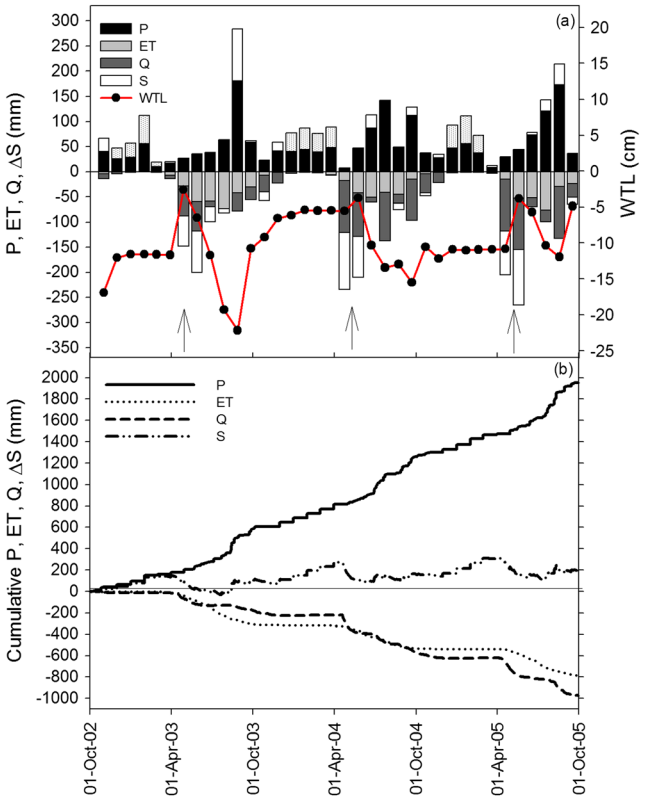

Figure 9. (a) Monthly partitioning of the mire water balance into precipitation (*P*), evapotranspiration (*ET*), discharge (*Q*), soil water storage change (Δ*S*), and water table level (*WTL*), and (b) cumulative daily *P*, *ET*, *Q*, and *S* from 1 October 2002 to 30 September 2005; note that during winter months, *S* represents snow accumulation; here positive fluxes (e.g., *P*) indicate water input, whereas negative fluxes (e.g., *ET*, *Q*) represent a water loss from the ecosystem; arrows indicate the timing of the snowmelt period.

Table 3. Non-growing Season (1 October to 30 April) to Growing Season (1 May to 30 September) Ratios of the Different Mire Water and Energy Balance Components (i.e., Net Radiation, R_n; Precipitation, *P*; Sensible Heat Flux, *H*; Latent Heat Flux, λE; and Discharge, *Q*, Derived From Weir Measurements) During the Hydrological Years 2000/2001–2004/2005

Year	R_n	*P*	*H*	λE	*Q*
2000/2001	−0.13	0.64	−0.74	0.19	N.A.
2001/2002	−0.18	0.55	−0.76	0.11	N.A.
2002/2003	−0.10	0.87	−0.48	0.13	0.68
2003/2004	−0.11	0.69	−0.58	0.12	0.58
2004/2005	−0.16	0.57	−0.77	0.10	0.59
Mean	−0.14	0.66	−0.67	0.13	0.61

that differences in R_n due to a latitudinal gradient is an important factor explaining differences in the energy partitioning between two peatlands located in different geographical regions.

[42] The 5 year mean growing season evaporative fraction (λE /R_n) of 0.63 was comparable to the 2 year mean of 0.60 reported for the ombrogenic mire Stormossen [*Kellner*, 2001] but higher compared to the range of 0.23 to 0.30 observed over 5 years in the Irish blanket bog [*Sottocornola and Kiely*, 2010]. Differences in the evaporative fraction among mires might result from both abiotic (e.g. T_a, *P*, *WTL*) and biotic (e.g. plant species composition, biomass, leaf area index) effects on either R_n or λE. In addition, the positive correlation between the evaporative fraction and R_n highlights the role of latitude (e.g., day length), cloud cover, and surface albedo as important controls on the fraction of R_n being partitioned into λE.

4.2. Characteristics and controls of mire evapotranspiration

4.2.1. Actual and potential evapotranspiration

[43] Maximum *ET* rates observed in our study were similar to those of several other peatlands [*Humphreys et al*., 2006; *Lafleur et al*., 2005; *Shimoyama et al*., 2003; *Sonnentag et al*., 2010] suggesting a common threshold of maximum *ET* in peatlands. Given the relatively narrow range in maximum LAI of commonly 1–2 $m^2 m^{-2}$ among contrasting peatlands [*Humphreys et al*., 2006], it is possible that physiological constraints on *ET* are rather similar despite differences in *WTL* (see also section 4.2.2) and composition of plant functional types. The low mean *ET*/*PET* ratio of 0.55 and Priestley-Taylor α values far below 1.26, which is characteristic for well-watered land surfaces [*Priestley and Taylor*, 1972], as well as the dominance of r_s over r_a, further highlights the importance of physiological constraints on *ET* even at this well-watered fen site. Similar observations and values for *ET*/*PET* and Priestley-Taylor α were reported for other peatland types and sites [*Humphreys et al*., 2006; *Lafleur et al*., 2005; *Sottocornola and Kiely*, 2010].

4.2.2. Surface conductance and water table level controls on evapotranspiration

[44] Surface conductance acts as a main regulator of the plant mediated water transport from the soil to the atmosphere [*Schulze et al*., 1994]. Overall, the daily range and the mean of the growing season surface conductance (g_s) at Degerö Stormyr were comparable to those reported in other peatlands [e.g., *Lloyd et al*., 2001; *Sottocornola and Kiely*, 2010]. However, micrometeorological measurements represent a bulk estimate of g_s that includes contributions from both moss and vascular plant communities and previous studies have highlighted that the relative composition of these contrasting plant communities has a crucial effect on magnitudes and patterns of g_s and *ET* [*Humphreys et al*., 2006; *Kurbatova et al*., 2002; *Lafleur*, 2008]. This is due to the fundamental difference that moss conductance is mainly regulated by water availability and leaf wetness whereas vascular plant conductance is primarily controlled by their stomatal response to radiation and *D* [*Kurbatova et al*., 2002; *Schulze et al*., 1994; *Williams and Flanagan*, 1996]. At the Degerö mire, vascular plants and mosses account each for approximately half of the photosynthetic active ecosystem biomass, [*Laine et al*., 2012]. Thus, the vascular plant fraction likely dominated the total ecosystem conductance and explained the R_g dependent response of g_s to *D* at low *D* levels at this site. In contrast, stomata closure and moss desiccation occurring during dry periods may have constrained the g_s response to R_g at increasing *D* levels. Furthermore, moss conductance has been reported to increase with surface roughness due to enhanced turbulent eddy flow into the canopy [*Rice et al*., 2001]. In contrast, we

observed a decrease in g_s (i.e., an increase in r_s) with increasing surface roughness length (z_0) over the growing season which further indicates a dominant role of the vascular plant community as control on g_s and *ET* at this site.

[45] The role of *WTL* on peatland *ET* is still subject to discussion [*Lafleur et al*., 2005; *Sonnentag et al*., 2010]. While the negative response of g_s to *WTL* observed in our study can be linked to the negative effects of reduced moss moisture content and water availability to vascular plant roots [*Schulze et al*., 1994; *Williams and Flanagan*, 1996], it is noteworthy that this response of g_s to *WTL* did not significantly affect *ET* as demonstrated by the lack of correlation between *WTL* and *ET*/*PET* in our study, which is in contrast to previous studies [*Bridgham et al*., 1999; e.g. *Kellner*, 2001; *Kim and Verma*, 1996]. The observed relationship of greater daily *ET* at lower *WTL* was due to the confounding effect with T_a, as high T_a, *D* (and thus high *ET*) and low *WTL* coincide during the summer period (and this pattern disappeared after accounting for T_a). Moreover, although daily *ET* leveled out at $D > 1$kPa, a reduction of *ET* at high *D* levels did not occur which indicates that sufficient soil water was available to maintain high *ET* rates even during dry conditions with low *WTL*. Similar to our findings, *ET* and *ET*/*PET* was not significantly affected by *WTL* in other peatlands with shallow (i.e., 0 to −30 cm) *WTL* [*Humphreys et al*., 2006; *Sonnentag et al*., 2010; *Sottocornola and Kiely*, 2010; *Wu et al*., 2010]. However, a significant reduction of *ET* and *ET*/*PET* occurred below a *WTL* of −60 cm in the ombotrophic Mer Bleu bog in relation to reduced water availability for both moss and vascular plant vegetation and the hydraulic properties of peat [*Lafleur et al*., 2005]. Thus, capillary forces by Sphagnum mosses and root access of vascular plants to a critical depth may be able to maintain wet ground surface conditions over a wide range of *WTL* and thereby explain the convergence of maximum daily *ET* (see section 4.2.1) and the lack of response of *ET* to shallow *WTL* fluctuations.

[46] The 5 year mean of annual *ET* at Degerö Stormyr (241 ± 48 mm) was close to the 2 year mean of 320 mm in a Finish mire [*Wu et al*., 2010] but considerably lower than the 5 year means of 476 mm at the raised bog Mer Bleue in southern Canada with deeper *WTL* [*Lafleur et al*., 2005] and of 394 mm in an Irish blanket bog with higher *WTL* [*Sottocornola and Kiely*, 2010]. Possible reasons for higher *ET* at these two peatlands compared to Degerö Stormyr may include the latitudinal effect on R_n, a warmer (milder winter in the case of the maritime Irish blanket bog) and longer growing season, higher *P* input at the Irish bog, and a denser cover of vascular plants at the Mer Bleu bog. Differences in the composition and seasonality of the plant canopies also accounted for much of the observed differences in *ET* between bog and fen mesocosms in the study of *Bridgham et al*. [1999]. Thus, climate and vegetation composition are likely stronger controls on annual *ET* than *WTL* alone across different mire types.

4.3. Controls and temporal patterns of the water budget components

[47] The partitioning of the water input into the different water budget components is important for determining nutrient accumulation and peatland development [*Eppinga et al*., 2010; *Nungesser*, 2003; *Pastor et al*., 2002]. The cumulative sums of measured *Q* and ΔS at our mire (174 to 404 mm and −95 to 89 mm, respectively) were comparable to those over 2 years at a boreal mire in Eastern Finland (194 to 387 mm and −50 to −20 mm, respectively) [*Wu et al*., 2010]. The relatively high *Q*/*P* ratio of 0.65 at Degerö Stormyr classifies this site as primarily drainage-driven peatland [*Eppinga et al*., 2010]. Nevertheless, contrasting temporal patterns of the partitioning between the water flux components were observed with *Q* being more important in spring and autumn while *ET* was greater during summer. Furthermore, the large inter-annual variation of the *Q*/*P* ratio (0.38 to 0.80) indicates the sensitivity of the mire water balance to various controls and internal feedbacks. For instance, the correlations of *ET*/*P* and *Q*/*P* with R_n suggest that controls of R_n (i.e., latitude, albedo, cloud cover, and vegetation structure) also affect the partitioning of the water budget. Similarly, the observed correlation between cumulative *P* and its partitioning into *Q* and *ET* has important implications given the large inter-annual variability observed in *P*. Furthermore, our findings highlight the role of *WTL* in determining whether precipitation events resulted in recharge of soil storage or increased runoff. Thus, in support of our second hypothesis, the water budget partitioning does not only depend on magnitudes but also on the frequency and timing of water input and concurrent *WTL* levels. An improved understanding of the controls determining variations in discharge is important because of its link to mire nutrient and carbon distribution and export dynamics [*Eppinga et al*., 2010; *Koehler et al*., 2011; *Nilsson et al*., 2008; *Roulet et al*., 2007].

4.4. The importance of non-growing season energy exchange and mire water budget partitioning in northern boreal landscapes

[48] Previous studies on peatland energy exchange have been often limited to the growing season period [e.g., *Humphreys et al*., 2006; *Kurbatova et al*., 2002; *Sonnentag et al*., 2010]. However, considering the long winter periods in boreal regions, it is important to understand how non-growing season energy exchange processes affect land surface energy balances [*Harding and Pomeroy*, 1996; *Kuusisto*, 1986; *Neumann and Marsh*, 1998]. The relatively small (12%) contribution of non-growing season λE to the annual sum at our site resulted essentially from fluxes occurring during snow-free periods in April and October/November (here defined as part of the non-growing season) and was therefore determined by the timing of spring snowmelt and autumn snowfall. Similar small but significant (10% and 25% of the annual sum, respectively) winter λE was previously reported for a Finnish mire [*Wu et al*., 2010] and a Canadian bog [*Lafleur et al*., 2005]. In comparison, non-growing season *H* was substantial and able to offset about two thirds of the growing season *H*. The large variations in *H* during the winter may be related to the thawing and freezing of the snow pack with the subsequent consumption and release of energy [*Kuusisto*, 1986; *Neumann and Marsh*, 1998]. Furthermore, ground heat fluxes during pre-melt conditions were reported to contribute about 25% to the total energy balance in peatland [*Knox et al*., 2012]. While winter measurements of Q are commonly quantified for snow-free periods only [e.g. *Wu et al*., 2010], the small but significant (10% of the annual sum) base flow observed during the snow covered period at our site demonstrate the need for

year-round measurements of Q using heated weirs [*Nilsson et al*., 2008; *Roulet et al*., 2007]. Overall, our findings confirm our third main hypothesis that non-growing season energy and water fluxes represent a significant portion of their annual exchanges in this northern boreal peatland. Snow cover and soil frost dynamics during the winter season may therefore act as important controls on the annual energy budgets in boreal peatlands.

[49] Within the context of boreal landscape ecology, it is also important to understand water budget dynamics during winter periods and the contribution of northern mire ecosystems to the landscape water balance [*Ågren et al*., 2007; *Buffam et al*., 2007; *Laudon et al*., 2004, 2007]. The dynamics of Q at our mire site were dominated by the spring snow melt, during which time the water input in the form of snow melt was close to that of Q. This is in contrast to forested ecosystems in the surrounding region where the snow melt period constitutes an important phase of soil recharge and is followed by substantially lower spring runoff [*Laudon et al*., 2004, 2007]. Thus, the presence of mire ecosystems may considerably modify the energy balance and water cycle of forested boreal catchments which highlights the need for inclusion of wetlands in regional and global climate models [*Lafleur*, 2008].

5. Conclusions

[50] We determined patterns and controls of the seasonal and inter-annual variability of energy and water fluxes in a minerogenic oligotrophic mire over 5 years (2001 to 2005) using eddy-covariance and weir discharge measurements. Based on our findings we conclude that

- Seasonal and inter-annual variations in the energy partitioning (i.e. the Bowen ratio) were mainly driven by changes in the latent heat flux which was also the dominant turbulent energy flux in terms of magnitude.
- Evapotranspiration, ET, was not directly related to water table level but instead primarily driven by changes in vapor pressure deficit and net radiation. We further conclude that significant physiological constraints on ET occurred in this well-watered fen.
- Seasonal and inter-annual variations of bulk surface conductance were strongly linked to water table level, vapor pressure deficit and net radiation which altogether affect magnitudes of the contrasting plant functional type- and species-specific conductance. However, while surface conductance was an important control on the diurnal ET patterns, its effect on ET was less pronounced on the season scale.
- The seasonal and annual partitioning of the mire water budget components was regulated by the amount and timing of net radiation and precipitation as well as by the concurrent water table level. Specifically, the mire water discharge was mainly controlled by the degree of saturation of the soil water storage resulting in episodic runoff during periods with high water table, i.e., during spring and autumn.
- Non-growing season energy exchanges, water fluxes, and water budget partitioning in northern mires are of significance for annual budgets in the boreal region.

[51] **Acknowledgments.** This study was financed by the Swedish Research Council for Environment, Agricultural Sciences and Spatial Planning (grant no. 21.4/2003-0876) and the Swedish Research Council (grant no. 621-2003-2730). We also acknowledge the Kempe Foundation for the grants supporting the micrometeorological instrumentation. This study is a contribution from the Nordic Center for Studies of Ecosystem Carbon Exchange and its Interactions with the Climate System (NECC) which is funded by the Nordic Council of Ministers.

References

Admiral, S. W., P. M. Lafleur, and N. T. Roulet (2006), Controls on latent heat flux and energy partitioning at a peat bog in eastern Canada, *Agr. Forest. Meteorol.*, *140*(1–4), 308–321, doi:10.1016/j.agrformet.2006.03.017.

Ågren, A., I. Buffam, M. Jansson, and H. Laudon (2007), Importance of seasonality and small streams for the landscape regulation of dissolved organic carbon export, *J. Geophys. Res.*, *112*(G3), G03003, doi:10.1029/2006JG000381.

Alexandersson, H., C. Karlström, and S. Larsson-McCann (1991), *Temperaturen och nedercörden i sverige 1961–1990*, SMHI, The Swedish Meteorological and Hydrological Institute, Norrköping, Sweden.

Amiro, B. D. et al. (2006), Carbon, energy and water fluxes at mature and disturbed forest sites, Saskatchewan, Canada, *Agr. Forest. Meteorol.*, *136*(3–4), 237–251, doi:10.1016/j.agrformet.2004.11.012.

Aubinet, M. et al. (1999), Estimates of the annual net carbon and water exchange of forests: The EUROFLUX methodology, *Adv. Ecol. Res.*, *30*, 113–175.

Barr, A. G., G. van der Kamp, T. A. Black, J. H. McCaughey, and Z. Nesic (2012), Energy balance closure at the BERMS flux towers in relation to the water balance of the White Gull Creek watershed 1999–2009, *Agr. Forest. Meteorol.*, *153*(0), 3–13, doi:10.1016/j.agrformet.2011.05.017.

Belyea, L. R., and A. J. Baird (2006), "The limits to peat bog growth": Cross-scale feedback in peatland development, *Ecol. Monogr.*, *76*, 299–322.

Belyea, L. R., and R. S. Clymo (2001), Feedback control of the rate of peat formation, *Proc. R. Soc. Lond. B*, *268*(1473), 1315–1321, doi:10.1098/rspb.2001.1665.

Bridgham, S. D., J. Pastor, K. Updegraff, T. J. Malterer, K. Johnson, C. Harth, and J. Chen (1999), Ecosystem control over temperature and energy flux in northern peatlands, *Ecol. Appl.*, *9*(4), 1345–1358, doi:10.1890/1051-0761(1999)009[1345:ECOTAE]2.0.CO;2.

Buffam, I., H. Laudon, J. Temnerud, C.-M. Mörth, and K. Bishop (2007), Landscape-scale variability of acidity and dissolved organic carbon during spring flood in a boreal stream network, *J. Geophys. Res.*, *112*, 11, doi:10.1029/2006JG000218.

Eppinga, M. B., M. Rietkerk, L. R. Belyea, M. B. Nilsson, P. C. Ruiter, and M. J. Wassen (2010), Resource contrast in patterned peatlands increases along a climatic gradient, *Ecology*, *91*(8), 2344–2355.

Eriksson, B. (1983), *Data Concerning the Precipitation Climate of Sweden, Mean Values for the Period 1951–80*, SMHI, The Swedish Meteorological and Hydrological Institute, Norrköping, Sweden.

Eugster, W. et al. (2000), Land–atmosphere energy exchange in Arctic tundra and boreal forest: available data and feedbacks to climate, *Glob. Chang. Biol.*, *6*(S1), 84–115, doi:10.1046/j.1365-2486.2000.06015.x.

Flanagan, L. B., and K. H. Syed (2011), Stimulation of both photosynthesis and respiration in response to warmer and drier conditions in a boreal peatland ecosystem, *Glob. Chang. Biol.*, *117*(7), 2271–2287, doi:10.1111/j.1365-2486.2010.02378.x.

Harding, R. J., and J. W. Pomeroy (1996), The energy balance of the winter boreal landscape, *J. Climate*, *9*(11), 2778–2787, doi:10.1175/1520-0442(1996)009<2778:TEBOTW>2.0.CO;2.

Humphreys, E. R., P. M. Lafleur, L. B. Flanagan, N. Hedstrom, K. H. Syed, A. J. Glenn, and R. Granger (2006), Summer carbon dioxide and water vapor fluxes across a range of northern peatlands, *J. Geophys. Res.*, *111*, 16, doi:10.1029/2005JG000111.

Ivanov, K. E. (1981), *Water Movement in Mirelands*, Translated from Russian by A. Thomson and H. A. P. Ingram, Academic Press, New York, NY.

Kellner, E. (2001), Surface energy fluxes and control of evapotranspiration from a Swedish Sphagnum mire, *Agr. Forest. Meteorol.*, *110*(2), 101–123, doi:10.1016/S0168-1923(01)00283-0.

Kim, J., and S. B. Verma (1996), Surface exchange of water vapour between an open sphagnum fen and the atmosphere, *Bound.-Layer Meteorol.*, *79*(3), 243–264, doi:10.1007/BF00119440.

Knox, S. H., S. K. Carey, and E. R. Humphreys (2012), Snow surface energy exchanges and snowmelt in a shrub-covered bog in eastern Ontario, Canada, *Hydrological Processes*, *26*(12), 1876–1890, doi:10.1002/hyp.9289.

Koehler, A.-K., M. Sottocornola, and G. Kiely (2011), How strong is the current carbon sequestration of an Atlantic blanket bog?, *Glob. Chang. Biol.*, *17*(1), 309–319, doi:10.1111/j.1365-2486.2010.02180.x.

Kurbatova, J., A. Arneth, N. N. Vygodskaya, O. Kolle, A. V. Varlargin, I. M. Milyukova, N. M. Tchebakova, E.-D. Schulze, and J. Lloyd (2002), Comparative ecosystem-atmosphere exchange of energy and mass in a European Russian and a central Siberian bog I. Interseasonal and interannual variability of energy and latent heat fluxes during the snowfree period, *Tellus B*, *54*(5), 497–513, doi:10.1034/j.1600-0889.2002.01354.x.

Kuusisto, E. (1986), The energy balance of a melting snow cover in different environments, *IAHS Publ.*, (*155*), 37–45.

Lafleur, P. M. (2008), Connecting atmosphere and wetland: Energy and water vapour exchange, *Geography Compass*, *2*(4), 1027–1057, doi:10.1111/j.1749-8198.2007.00132.x.

Lafleur, P. M., R. A. Hember, S. W. Admiral, and N. T. Roulet (2005), Annual and seasonal variability in evapotranspiration and water table at a shrub-covered bog in southern Ontario, Canada, *Hydrological Processes*, *19*(18), 3533–3550, doi:10.1002/hyp.5842.

Lafleur, P. M., J. H. McCaughey, D. W. Joiner, P. A. Bartlett, and D. E. Jelinski (1997), Seasonal trends in energy, water, and carbon dioxide fluxes at a northern boreal wetland, *J. Geophys. Res.*, *102*(D24), 29,009–29,020, doi:10.1029/96JD03326.

Laine, A. M., J. Bubier, T. Riutta, M. B. Nilsson, T. R. Moore, H. Vasander, and E. S. Tuittila (2012), Abundance and composition of plant biomass as potential controls for mire net ecosytem CO_2 exchange, *Botany*, *90*(1), 63–74, doi:10.1139/b11-068.

Laudon, H., J. Seibert, S. Köhler, and K. Bishop (2004), Hydrological flow paths during snowmelt: Congruence between hydrometric measurements and oxygen 18 in meltwater, soil water, and runoff, *Water Resour. Res.*, *40*, 9, doi:10.1029/2003WR002455.

Laudon, H., V. Sjöblom, I. Buffam, J. Seibert, and M. Mörth (2007), The role of catchment scale and landscape characteristics for runoff generation of boreal streams, *J. Hydrol.*, *344*(3–4), 198–209, doi:10.1016/j.jhydrol.2007.07.010.

Lloyd, C. R., R. J. Harding, T. Friborg, and M. Aurela (2001), Surface fluxes of heat and water vapour from sites in the European Arctic, *Theor. Appl. Climatol.*, *70*(1–4), 19–33, doi:10.1007/s007040170003.

Mölder, M., and E. Kellner (2002), Excess resistance of bog surfaces in central Sweden, *Agr. Forest. Meteorol.*, *112*(1), 23–30, doi:10.1016/S0168-1923(02)00043-6.

Moncrieff, J. b., Y. Malhi, and R. Leuning (1996), The propagation of errors in long-term measurements of land-atmosphere fluxes of carbon and water, *Glob. Chang. Biol.*, *2*(3), 231–240, doi:10.1111/j.1365-2486.1996.tb00075.x.

Monteith, J. L. (1965), Evaporation and environment, *Symp. Soc. Exp. Biol.*, *19*, 205–234.

Morgenstern, K., T. A. Black, E. R. Humphreys, T. J. Griffis, G. B. Drewitt, T. Cai, Z. Nesic, D. L. Spittlehouse, and N. J. Livingston (2004), Sensitivity and uncertainty of the carbon balance of a Pacific Northwest Douglas-fir forest during an El Niño/La Niña cycle, *Agr. Forest. Meteorol.*, *123*(3–4), 201–219.

Neumann, N., and P. Marsh (1998), Local advection of sensible heat in the snowmelt landscape of Arctic tundra, *Hydrological Processes*, *12*(10-11), 1547–1560, doi:10.1002/(SICI)1099-1085(199808/09)12:10/11<1547::AID-HYP680>3.0.CO;2-Z.

Nilsson, M., J. Sagerfors, I. Buffam, H. Laudon, T. Eriksson, A. Grelle, L. Klemedtsson, P. Weslien, and A. Lindroth (2008), Contemporary carbon accumulation in a boreal oligotrophic minerogenic mire—A significant sink after accounting for all C-fluxes, *Glob. Chang. Biol.*, *14*(10), 2317–2332, doi:10.1111/j.1365-2486.2008.01654.x.

Nordbakken, J.-F. (1996), Plant niches along the water-table gradient on an ombrotrophic mire expanse, *Ecography*, *19*(2), 114–121.

Nungesser, M. K. (2003), Modelling microtopography in boreal peatlands: Hummocks and hollows, *Ecol. Model.*, *165*(2–3), 175–207, doi:10.1016/S0304-3800(03)00067-X.

Paavalainen, E., and J. Päivinen (1995), *Peatland Forestry: Ecology and Principles*, Springer, Berlin.

Pastor, J., B. Peckham, S. Bridgham, J. Weltzin, and J. Chen (2002), Plant community dynamics, nutrient cycling, and alternative stable equilibria in peatlands, *Am. Nat.*, *160*(5), 553–568, doi:10.1086/342814.

Priestley, C. H. B., and R. J. Taylor (1972), On the assessment on surface heatflux and evaporation using large-scale parameters, *Monthly Weather Rev.*, *100*, 81–92.

Rice, S. K., D. Collins, and A. M. Anderson (2001), Functional significance of variation in bryophyte canopy structure, *Am. J. Bot.*, *88*(9), 1568–1576.

Robroek, B., M. G. C. Schouten, J. Limpens, F. Berendse, and H. Poorter (2009), Interactive effects of water table and precipitation on net CO_2 assimilation of three co-occurring Sphagnum mosses differing in distribution above the water table, *Glob. Chang. Biol.*, *15*(3), 680–691, doi:10.1111/j.1365-2486.2008.01724.x.

Roulet, N., S. Hardill, and N. Comer (1991), Continuous measurement of the depth of water table (inundation) in wetlands with fluctuating surfaces, *Hydrological Processes*, *5*(4), 399–403, doi:10.1002/hyp.3360050407.

Roulet, N. T., P. M. Lafleur, P. J. H. Richard, T. R. Moore, E. R. Humphreys, and J. Bubier (2007), Contemporary carbon balance and late Holocene carbon accumulation in a northern peatland, *Glob. Chang. Biol.*, *13*(2), 397–411, doi:10.1111/j.1365-2486.2006.01292.x.

Rouse, W. R. (2000), The energy and water balance of high-latitude wetlands: Controls and extrapolation, *Glob. Chang. Biol.*, *6*(S1), 59–68, doi:10.1046/j.1365-2486.2000.06013.x.

Rydin, H., and A. J. S. McDonald (1985a), Photosynthesis in Sphagnum at different water contents, *J. Bryol.*, *13*, 579–584.

Rydin, H., and A. J. S. McDonald (1985b), Tolerance of Sphagnum to water level, *J. Bryol.*, *13*, 571–578.

Sagerfors, J., A. Lindroth, A. Grelle, L. Klemedtsson, P. Weslien, and M. Nilsson (2008), Annual CO_2 exchange between a nutrient-poor, minerotrophic, boreal mire and the atmosphere, *J. Geophys. Res.*, *113*(G1), doi:10.1029/2006JG000306.

Schmid, H. P. (1994), Source areas for scalars and scalar fluxes, *Bound.-Layer Meteorol.*, *67*(3), 293–318, doi:10.1007/BF00713146.

Schulze, E., F. M. Kelliher, C. Korner, J. Lloyd, and R. Leuning (1994), Relationships among maximum stomatal conductance, ecosystem surface conductance, carbon assimilation rate, and plant nitrogen nutrition: A global ecology scaling exercise, *Annu. Rev. Ecol. Syst.*, *25*(1), 629–662, doi:10.1146/annurev.es.25.110194.003213.

Shimoyama, K., T. Hiyama, Y. Fukushima, and G. Inoue (2003), Seasonal and interannual variation in water vapor and heat fluxes in a West Siberian continental bog, *J. Geophys. Res.*, *108*, 13, doi:10.1029/2003JD003485.

Sonnentag, O., G. van der Kamp, A. G. Barr, and J. M. Chen (2010), On the relationship between water table depth and water vapor and carbon dioxide fluxes in a minerotrophic fen, *Glob. Chang. Biol.*, *16*(6), 1762–1776, doi:10.1111/j.1365-2486.2009.02032.x.

Sottocornola, M., and G. Kiely (2010), Energy fluxes and evaporation mechanisms in an Atlantic blanket bog in southwestern Ireland, *Water Resour. Res.*, *46*, 13, doi:10.1029/2010WR009078.

Verma, S. B. (1989), Aerodynamic resistances to transfers of heat, mass and momentum, in *Estimation of Areal Evapotranspiration*, edited by T. A. Black *et al*., pp. 13–20, Int. Assoc. Hydrol. Sci., Vancouver, B.C.

Williams, C. A. et al. (2012), Climate and vegetation controls on the surface water balance: Synthesis of evapotranspiration measured across a global network of flux towers, *Water Resour. Res.*, *48*(6), W06523, doi:10.1029/2011WR011586.

Williams, T. G., and L. B. Flanagan (1996), Effect of changes in water content on photosynthesis, transpiration and discrimination against $^{13}CO_2$ and $C^{18}O^{16}O$ in Pleurozium and Sphagnum, *Oecologia*, *108*(1), 38–46.

Wu, J., L. Kutzbach, D. Jager, C. Wille, and M. Wilmking (2010), Evapotranspiration dynamics in a boreal peatland and its impact on the water and energy balance, *J. Geophys. Res.*, *115*, 18, doi:10.1029/2009JG001075.